

UTHEP-393

Perturbative Renormalization Factors of Quark Bilinear Operators for Domain-wall QCD

¹Sinya Aoki, ¹Taku Izubuchi, ²Yoshinobu Kuramashi ^{*} and ¹Yusuke Taniguchi

¹*Institute of Physics, University of Tsukuba, Tsukuba, Ibaraki 305-8571, Japan*

²*Department of Physics, Washington University, St. Louis, Missouri 63130, USA*

(February 1, 2008)

Abstract

We calculate one-loop renormalization factors of bilinear operators made of physical quark fields for domain-wall QCD. We find that finite parts of such renormalization factors have reasonable values at 1-loop except an overlap factor between the physical quark field and the zero mode in the theory. We point out that the 1-loop estimate of overall renormalization factors becomes unreliable at the coupling where numerical simulations are currently performed, due to the presence of this overlap factor. We show that this problem disappears if the mean-field improved perturbation theory is employed for renormalization factors.

Typeset using REVTEX

^{*}On leave from Institute of Particle and Nuclear Studies, High Energy Accelerator Research Organization(KEK), Tsukuba, Ibaraki 305-0801, Japan

I. INTRODUCTION

The lack of chirally invariant fermion formulations is one of the most uncomfortable points theoretically and practically in lattice QCD. For example, in the Wilson fermion formulation, which is popularly used in numerical simulations, the chiral limit can be realized only by the fine tuning of bare mass parameter, which compensates the additive quantum correction to the quark mass.

Recently the domain-wall fermion formulation [1,2], which was originally proposed for lattice chiral gauge theories [3], has been employed in lattice QCD simulations [4] and has shown its superiority over other formulations: there seems no need of the fine tuning to realize the chiral limit while there is no restriction to the number of flavors. In particular massless mode which presents at the tree level seems stable against the quantum correction. Since this property is not a trivial one, two of us have performed the perturbative calculation for the domain-wall quark propagator and have shown that the massless mode is indeed stable against the 1-loop correction [5]. The wave function renormalization factor for the massless mode has also been evaluated there.

In this paper we extend our previous perturbative calculation to an evaluation of renormalization factors for quark bilinear operators at 1-loop in domain-wall QCD. These renormalization factors are needed to convert matrix elements such as meson decay constants measured in lattice simulations to those in $\overline{\text{MS}}$ scheme, so that the values predicted on the lattice can be compared with the corresponding experimental values. In particular, in order to discuss the scaling behavior of such matrix elements, the correction by the renormalization factors becomes important, since 1-loop corrections are in general non-negligible at the gauge coupling used in simulations. Moreover since 1-loop corrections decrease only as the inverse of the logarithm of the lattice spacing, not a power of it, they can not be removed through the usual continuum extrapolation like linear or quadratic in the lattice spacing. Therefore the corrections by the renormalization factors to such matrix elements must be included for precise measurements in numerical simulations with the domain-wall QCD.

We start from the Green's function with quark bilinear operators and physical quark fields. We show that the divergence in the Green's function can be renormalized into the quark propagator and bilinear operators. There appears no mixing between these operators and operators made of heavy unphysical fermions. The renormalization factor consists of two parts, one is the usual renormalization factor which has similar value as that of Wilson fermion, another is the factor of overlap between field on each two boundary wall and the zero mode. We notice that this overlap factor is renormalized additively and tends to be large. We present renormalization factors with mean-field improvement to suppress this large correction.

This paper is organized as follows. In Sec. II we introduce the action of domain-wall QCD together with some notations used in this paper and explicitly give the Feynman rules relevant to our calculations. In Sec. III we evaluate the self-energy of the physical fermion, from which we extract the wave function renormalization factor of the physical fermion and the multiplicative mass renormalization factor. Although results for both wave function [5] and mass [6] renormalization factors have already been reported, we give them here in order to demonstrate our method of calculating renormalization factors in domain-wall QCD. In particular we pay attention to the extra factor in the wave function renormalization, which

arises as the overlap between the physical fermion field and the zero mode. We then calculate the renormalization factors for quark bilinear operators in Sec. IV. Numerical results of one-loop coefficients for various quantities are given in Sec. V as a function of M in both cases with and without the mean-field improvement. Our conclusion is given in Sec. VI.

In this paper we set the lattice spacing $a = 1$ and take $SU(N_c)$ gauge group with the gauge coupling g and the second Casimir $C_F = \frac{N_c^2 - 1}{2N_c}$.

II. ACTION AND FEYNMAN RULES

The domain-wall fermion is a 4+1 dimensional Wilson fermion with a “mass term” which depends on the coordinate in the extra dimension. For the explicit form of the “mass term” we adopt the Shamir’s one [1] in this paper and the quark action with the current quark mass m becomes

$$S_{\text{DW}} = \sum_n \sum_{s=1}^N \left[\frac{1}{2} \sum_\mu \left(\bar{\psi}(n)_s (-r + \gamma_\mu) U_\mu(n) \psi(n + \mu)_s + \bar{\psi}(n)_s (-r - \gamma_\mu) U_\mu^\dagger(n - \mu) \psi(n - \mu)_s \right) \right. \\ \left. + \frac{1}{2} \left(\bar{\psi}(n)_s (1 + \gamma_5) \psi(n)_{s+1} + \bar{\psi}(n)_s (1 - \gamma_5) \psi(n)_{s-1} \right) + (M - 1 + 4r) \bar{\psi}(n)_s \psi(n)_s \right] \\ + m \sum_n \left(\bar{\psi}(n)_N P_+ \psi(n)_1 + \bar{\psi}(n)_1 P_- \psi(n)_N \right), \quad (\text{II.1})$$

where n is a 4 dimensional space-time coordinate and s is an extra fifth dimensional index, the Dirac “mass” M is a parameter of the theory which we set $0 \leq M \leq 2$ to realize the massless fermion at tree level, m is a physical quark mass, and the Wilson parameter is set to $r = -1$. Our γ matrix convention is as follows:

$$\gamma_i = \begin{pmatrix} 0 & -i\sigma^i \\ i\sigma^i & 0 \end{pmatrix}, \quad \gamma_4 = \begin{pmatrix} 0 & 1 \\ 1 & 0 \end{pmatrix}, \quad \gamma_5 \equiv \gamma_1 \gamma_2 \gamma_3 \gamma_4 = \begin{pmatrix} 1 & 0 \\ 0 & -1 \end{pmatrix}, \quad (\text{II.2})$$

$$P_\pm = \frac{1 \pm \gamma_5}{2}, \quad (\text{II.3})$$

$$\sigma_{\mu\nu} = \frac{1}{2} [\gamma_\mu, \gamma_\nu]. \quad (\text{II.4})$$

The gauge part of the domain-wall fermion is a standard 4 dimensional one plaquette action and we have no gauge interaction along the fifth dimension. We can interpret this fifth dimensional degrees of freedom as a flavor [7]. It is important to notice that we have boundaries for the flavor space; $1 \leq s \leq N$.

The remarkable property of the domain-wall fermion is that there exists a massless fermion mode in the $N \rightarrow \infty$ limit at small momentum at $m = 0$. This massless fermion stays near the boundaries of the flavor space with the left and the right mode on the opposite side. At tree level the massless mode χ_0 is given explicitly in zero momentum limit as

$$\chi_0 = \sqrt{1 - w_0^2} \left(P_+ w_0^{s-1} \psi_s + P_- w_0^{N-s} \psi_s \right), \quad (\text{II.5})$$

where $w_0 = 1 - M$. Although the zero mode is stable against quantum correction [5], the damping factor w_0 is modified because the Dirac mass M is renormalized additively. In

numerical simulations it is more convenient to use the interpolating “physical” quark field defined by the boundary fermions

$$\begin{aligned} q(n) &= P_+ \psi(n)_1 + P_- \psi(n)_N, \\ \bar{q}(n) &= \bar{\psi}(n)_N P_+ + \bar{\psi}(n)_1 P_-. \end{aligned} \quad (\text{II.6})$$

We use the QCD operators constructed from this quark fields, since this field has been actually used in the previous simulations. Moreover, as seen later, we find that the renormalization becomes simpler for the operators in terms of the physical quark field.

Weak-coupling perturbation theory is developed by writing

$$U_{n,\mu} = \exp(igaA_\mu(n + \frac{1}{2}\hat{\mu})). \quad (\text{II.7})$$

Since our gauge part is same as that of the usual Wilson plaquette action, the gluon propagator can be written as

$$G_{\mu\nu}^{ab}(p) = \frac{1}{4 \sin^2 p/2} \left[\delta_{\mu\nu} - (1 - \alpha) \frac{4 \sin p_\mu/2 \sin p_\nu/2}{4 \sin^2 p/2} \right] \delta_{ab}, \quad (\text{II.8})$$

where $\sin^2 p/2 = \sum_\mu \sin^2 p_\mu/2$ and we set $\alpha = 1$ in our calculation. Quark-gluon vertices are also identical to those in the N flavor Wilson fermion. We employ the following two of those relevant for the one loop calculation:

$$V_{1\mu}^a(k, p)_{st} = -igT^a \{ \gamma_\mu \cos \frac{a}{2}(-k_\mu + p_\mu) - ir \sin \frac{a}{2}(-k_\mu + p_\mu) \} \delta_{st}, \quad (\text{II.9})$$

$$V_{2\mu\nu}^{ab}(k, p)_{st} = \frac{a}{2} g^2 \frac{1}{2} \{ T^a, T^b \} \{ i\gamma_\mu \sin \frac{a}{2}(-k_\mu + p_\mu) - r \cos \frac{a}{2}(-k_\mu + p_\mu) \} \delta_{\mu\nu} \delta_{st}. \quad (\text{II.10})$$

Our momentum assignments for the vertices are given in Fig. 1.

The fermion propagator is given by inverting the domain-wall Dirac operator, whose formula in momentum space is

$$\mathcal{D}(p)_{st} = \sum_\mu i\gamma_\mu \sin p_\mu \delta_{st} + (W^+(p) + mM^+)_{s,t} P_+ + (W^-(p) + mM^-)_{s,t} P_-, \quad (\text{II.11})$$

where the mass matrix is

$$W^+(p)_{s,t} = \begin{pmatrix} -W(p) & 1 & & \\ & -W(p) & \ddots & \\ & & \ddots & 1 \\ & & & -W(p) \end{pmatrix}, \quad (\text{II.12})$$

$$W^-(p)_{s,t} = \begin{pmatrix} -W(p) & & & \\ 1 & -W(p) & & \\ & \ddots & \ddots & \\ & & 1 & -W(p) \end{pmatrix}, \quad (\text{II.13})$$

$$M^+ = \begin{pmatrix} & & \\ & & \\ 1 & & \end{pmatrix}, \quad M^- = \begin{pmatrix} & 1 \\ & & \\ & & \end{pmatrix}, \quad (\text{II.14})$$

$$W(p) = 1 - M - r \sum_\mu (1 - \cos p_\mu). \quad (\text{II.15})$$

In numerical simulations one should take N large enough in order to have a massless quark in the spectrum at $m = 0$. This means that we can effectively neglect $e^{-\alpha N}$ terms with positive α . Therefore in our 1-loop calculation we will take $N \rightarrow \infty$ limit to avoid complications arising from the finite N . Although the $N \rightarrow \infty$ limit should be taken after the momentum integral in principle, it is easy to see that the limit can be taken before the integral. We may take the form of free fermion propagator in the $N \rightarrow \infty$ limit from the beginning. (See [5] for the derivation of the finite N fermion propagator.) Inverting (II.11) the fermion propagator for $N \rightarrow \infty$ becomes

$$\begin{aligned} S_F(p)_{st} &\equiv \left(\mathcal{P}(p)^{-1} \right)_{st} \\ &= \left(-i\gamma_\mu \sin p_\mu + W^- + mM^+ \right)_{su} G_R(u, t) P_+ \\ &\quad + \left(-i\gamma_\mu \sin p_\mu + W^+ + mM^- \right)_{su} G_L(u, t) P_-, \end{aligned} \quad (\text{II.16})$$

where sum over the same index is taken implicitly. $G_{R/L}$ is given by

$$G_R(s, t) = \frac{A}{F} \left[-(1-m^2) (1 - We^{-\alpha}) e^{\alpha(-2N+s+t)} - (1-m^2) (1 - We^\alpha) e^{-\alpha(s+t)} \right. \\ \left. - 2W \sinh(\alpha)m (e^{\alpha(-N+s-t)} + e^{\alpha(-N-s+t)}) \right] + Ae^{-\alpha|s-t|}, \quad (\text{II.17})$$

$$G_L(s, t) = \frac{A}{F} \left[-(1-m^2) (1 - We^\alpha) e^{\alpha(-2N+s+t-2)} - (1-m^2) (1 - We^{-\alpha}) e^{\alpha(-s-t+2)} \right. \\ \left. - 2W \sinh(\alpha)m (e^{\alpha(-N+s-t)} + e^{\alpha(-N-s+t)}) \right] + Ae^{-\alpha|s-t|}, \quad (\text{II.18})$$

$$\cosh(\alpha) = \frac{1 + W^2 + \sum_\mu \sin^2 p_\mu}{2W}, \quad (\text{II.19})$$

$$A = \frac{1}{2W \sinh(\alpha)}, \quad (\text{II.20})$$

$$F = 1 - e^\alpha W - m^2 (1 - We^{-\alpha}). \quad (\text{II.21})$$

Note that the argument p of factors α and W is suppressed in the above formula.

Besides the fermion propagator given above, the propagator for the physical quark field, defined in (II.6), is also used in this paper. The explicit form is rather simple and is given by

$$S_q(p) \equiv \langle q(-p) \bar{q}(p) \rangle = \frac{-i\gamma_\mu \sin p_\mu + (1 - We^{-\alpha}) m}{-(1 - e^\alpha W) + m^2(1 - We^{-\alpha})}. \quad (\text{II.22})$$

III. RENORMALIZATION FOR QUARK MASS AND WAVE FUNCTION

In this section we calculate the self energy for the physical quark field, from which we derive renormalization factors for mass and wave function. The physical quark propagator (II.22) at tree level becomes

$$S_q(p) = \frac{(1 - w_0^2)}{ip + (1 - w_0^2)m} \quad (\text{III.1})$$

in the continuum limit. In the following we will see that the full quark propagator with 1-loop corrections takes the following form:

$$S_q(p)_{\text{full}} = \frac{(1 - w_0^2) Z_w Z_2}{i\cancel{p} + (1 - w_0^2) Z_w Z_m^{-1} m}, \quad (\text{III.2})$$

where Z_2 and Z_m are the quark wave function and the mass renormalization factors respectively. In Ref. [5] Z_2 is calculated, while Z_m is given in Ref. [6]. Z_w , which is dropped in Ref. [5], is a renormalization factor for the overall factor $(1 - w_0^2)$.

One loop corrections to the quark two point function $\langle q(-p)\bar{q}(p) \rangle$ are given by two diagrams in Fig. 2. In the diagrams interaction vertices contain fermion field of a general flavor index, while physical quark field appears on the external lines. Tree-level propagators for the external lines are given by

$$\begin{aligned} \langle q(-p)\bar{\psi}(p, s) \rangle &= \frac{1}{F} \left(i\gamma_\mu \sin p_\mu - m (1 - We^{-\alpha}) \right) \left(e^{-\alpha(N-s)} P_+ + e^{-\alpha(s-1)} P_- \right) \\ &\quad + \frac{1}{F} \left[m \left(i\gamma_\mu \sin p_\mu - m (1 - We^{-\alpha}) \right) - F \right] e^{-\alpha} \left(e^{-\alpha(s-1)} P_+ + e^{-\alpha(N-s)} P_- \right), \end{aligned} \quad (\text{III.3})$$

$$\begin{aligned} \langle \psi(-p, s)\bar{q}(p) \rangle &= \frac{1}{F} \left(e^{-\alpha(N-s)} P_- + e^{-\alpha(s-1)} P_+ \right) \left(i\gamma_\mu \sin p_\mu - m (1 - We^{-\alpha}) \right) \\ &\quad + \frac{1}{F} \left(e^{-\alpha(s-1)} P_- + e^{-\alpha(N-s)} P_+ \right) e^{-\alpha} \left[m \left(i\gamma_\mu \sin p_\mu - m (1 - We^{-\alpha}) \right) - F \right]. \end{aligned} \quad (\text{III.4})$$

In the one loop calculation we take external momenta and quark masses much smaller than the lattice cut-off, so that we can expand the propagator corresponding to external lines in terms of external momenta and masses. In diagrams in Fig. 2 it is enough for the renormalization to expand the external propagator to the next to leading order,

$$\begin{aligned} \langle q(-p)\bar{\psi}(p, s) \rangle &\rightarrow \frac{1 - w_0^2}{i\cancel{p} + (1 - w_0^2)m} \left[\left(w_0^{(N-s)} P_+ + w_0^{(s-1)} P_- \right) - \frac{w_0}{1 - w_0^2} i\cancel{p} \left(w_0^{(s-1)} P_+ + w_0^{(N-s)} P_- \right) \right], \end{aligned} \quad (\text{III.5})$$

$$\begin{aligned} \langle \psi(-p, s)\bar{q}(p) \rangle &\rightarrow \left[\left(w_0^{(N-s)} P_- + w_0^{(s-1)} P_+ \right) - \left(w_0^{(s-1)} P_- + w_0^{(N-s)} P_+ \right) \frac{w_0}{1 - w_0^2} i\cancel{p} \right] \frac{1 - w_0^2}{i\cancel{p} + (1 - w_0^2)m}. \end{aligned} \quad (\text{III.6})$$

Note that both terms at the leading and the next to leading orders in the external propagator give the leading order contribution in these diagrams since interaction vertices have the form $a + bp_\mu$ due to the Wilson term.

The external propagator has the characteristic form in the continuum limit that it consists of the quark propagator times some dumping factor. One loop correction to the quark propagator becomes

$$\langle q(-p)\bar{q}(p) \rangle_1 = \frac{1 - w_0^2}{i\cancel{p} + (1 - w_0^2)m} \Sigma_q(p, m) \frac{1 - w_0^2}{i\cancel{p} + (1 - w_0^2)m}, \quad (\text{III.7})$$

which is easily renormalized into the quark propagator. Here $\Sigma_q(p, m)$ is given by multiplying the fermion self energy $\Sigma(p, m)_{st}$ by the factors in the external propagator,

$$\begin{aligned}\Sigma_q(p, m) = & \left[\left(w_0^{(N-s)} P_+ + w_0^{(s-1)} P_- \right) - \frac{w_0}{1-w_0^2} i\gamma^\mu \left(w_0^{(s-1)} P_+ + w_0^{(N-s)} P_- \right) \right] \Sigma(p, m)_{st} \\ & \times \left[\left(w_0^{(N-t)} P_- + w_0^{(t-1)} P_+ \right) - \left(w_0^{(t-1)} P_- + w_0^{(N-t)} P_+ \right) \frac{w_0}{1-w_0^2} i\gamma^\mu \right].\end{aligned}\quad (\text{III.8})$$

Calculating the quark self-energy $\Sigma(p, m)_{st}$ to one-loop order and making an expansion of the form

$$\Sigma(p, m)_{st} = \Sigma(0)_{st} + \frac{\partial \Sigma(0)_{st}}{\partial p_\mu} p_\mu + \frac{\partial \Sigma(0)_{st}}{\partial m} m + O(p^2, m^2, pm), \quad (\text{III.9})$$

we find

$$\Sigma(p, m)_{st} = -g^2 C_F \left[i\gamma^\mu \left(I^+ P_+ + I^- P_- \right) + W_1^+ P_+ + W_1^- P_- + m \left(M_1^+ P_+ + M_1^- P_- \right) \right]_{st}, \quad (\text{III.10})$$

where I^\pm and W_1^\pm are already calculated in our previous paper [5] for the massless fermion,

$$\begin{aligned}I_{st}^{+/-} = & -\frac{T}{2} \delta_{st} + \frac{1}{16\pi^2} (C_{+/-})_{s,t} \left(\ln(\pi^2) - 1 - \ln \lambda^2 \right) \\ & + \int \frac{d^4 l}{(2\pi)^4} \frac{1}{4 \sin^2 l/2} \left[\frac{1}{8} \sum_\mu \left(\cos l_\mu (W^- G_R + W^+ G_L)(s, t) + \sin^2 l_\mu (G_L + G_R)(s, t) \right) \right. \\ & + \sum_\mu \frac{\sin^2 l_\mu}{4(4 \sin^2 l/2)^2} \left((W^- G_R + W^+ G_L)(s, t) + 2 \left(\sum_\nu \cos^2 \frac{l_\nu}{2} - 2 \cos^2 \frac{l_\mu}{2} \right) G_{L/R}(s, t) \right. \\ & \left. \left. + \sum_\nu \sin^2 \frac{l_\nu}{2} G_{R/L}(s, t) \right) \right] - (C_{+/-})_{s,t} \int \frac{d^4 l}{(2\pi)^4} \frac{1}{(l^2)^2} \theta(\pi^2 - l^2),\end{aligned}\quad (\text{III.11})$$

$$\begin{aligned}(W_1^{+/-})_{s,t} = & -2T \delta_{st} + \int \frac{d^4 l}{(2\pi)^4} \frac{1}{4 \sin^2 l/2} \sum_\mu \left[\cos^2 \frac{l_\mu}{2} (W^{+/-} G_{L/R})(s, t) \right. \\ & \left. - \sin^2 \frac{l_\mu}{2} (W^{-/+} G_{R/L})(s, t) + \frac{1}{2} \sin^2 l_\mu (G_L + G_R)(s, t) \right].\end{aligned}\quad (\text{III.12})$$

Here T is the tadpole loop integral

$$T = \int_{-\pi}^{\pi} \frac{d^4 l}{(2\pi)^4} \frac{1}{4 \sin^2 \frac{l}{2}} = 0.15493. \quad (\text{III.13})$$

Note that the notation used in this paper is slightly different from that in Ref. [5]. In particular the infrared divergence in the loop integral is regularized by a gluon mass λ introduced in the gluon propagator in this paper, while the external fermion momentum is kept non-zero in Ref. [5] to avoid such an infrared divergence. The calculation becomes simpler in the former.

It is also straightforward to calculate one loop correction to mass term M_1^\pm ,

$$(M_1^{+/-})_{s,t} = \frac{4}{16\pi^2} (B_{+/-})_{s,t} \left(\ln(\pi^2) - \ln \lambda^2 \right)$$

$$\begin{aligned}
& + \int \frac{d^4 l}{(2\pi)^4} \frac{1}{4 \sin^2 l/2} \sum_{\mu} \left[\cos^2 \frac{l_{\mu}}{2} \left(W^{+/-} \frac{\partial G_{L/R}}{\partial m} + M^{+/-} G_{L/R} \right) (s, t) \right. \\
& - \sin^2 \frac{l_{\mu}}{2} \left(W^{-/+} \frac{\partial G_{R/L}}{\partial m} + M^{-/+} G_{R/L} \right) (s, t) + \frac{1}{2} \sin^2 l_{\mu} \left(\frac{\partial G_L}{\partial m} + \frac{\partial G_R}{\partial m} \right) (s, t) \left. \right] \\
& - (B_{+/-})_{s,t} 4 \int \frac{d^4 l}{(2\pi)^4} \frac{1}{(l^2)^2} \theta(\pi^2 - l^2),
\end{aligned} \tag{III.14}$$

where $C_{+/-}$ and $B_{+/-}$ are defined by

$$(C_+)_st = (1 - w_0^2)w_0^{s+t-2}, \quad (C_-)_st = (1 - w_0^2)w_0^{2N-s-t}, \tag{III.15}$$

$$(B_+)_st = (1 - w_0^2)^2 w_0^{N-s+t-1}, \quad (B_-)_st = (1 - w_0^2)^2 w_0^{s-1+N-t}. \tag{III.16}$$

Substituting these into (III.8) and neglecting higher order terms of $\mathcal{O}(p^2, m^2, pm)$ we obtain

$$\begin{aligned}
\Sigma_q(p, m) = & -\frac{1}{1 - w_0^2} i \not{p} \frac{g^2 C_F}{16\pi^2} \left[(-\log \lambda^2 a^2 - \Sigma_1) + \frac{2w_0}{1 - w_0^2} \Sigma_3 \right] \\
& - m \frac{g^2 C_F}{16\pi^2} (-4 \log \lambda^2 a^2 - \Sigma_2),
\end{aligned} \tag{III.17}$$

where

$$\Sigma_1 = -\log \pi^2 + 1 + \left(\frac{T}{2} - I^d \right) \cdot 16\pi^2, \tag{III.18}$$

$$\Sigma_2 = -4 \log \pi^2 - \sigma_m \cdot 16\pi^2, \tag{III.19}$$

$$\Sigma_3 = (2T - \tilde{\omega}) \cdot 16\pi^2, \tag{III.20}$$

$$\begin{aligned}
I^d = & \int \frac{d^4 l}{(2\pi)^4} \left\{ \frac{1}{32 \sin^2 l/2} \sum_{\mu} \left[\sin^2 l_{\mu} (\tilde{G}_R + \tilde{G}_L) + 2 \cos l_{\mu} (w_0 - W) \tilde{G}_R \right] \right. \\
& + \sum_{\mu} \frac{\sin^2 l_{\mu}}{2(4 \sin^2 l/2)^2} \left[(w_0 - W) \tilde{G}_R + \left(\sum_{\nu} \cos^2 l_{\nu}/2 - 2 \cos^2 l_{\mu}/2 \right) \tilde{G}_L + \sum_{\nu} (\sin^2 l_{\nu}/2) \tilde{G}_R \right] \\
& \left. - \frac{1}{(l^2)^2} \theta(\pi^2 - l^2) \right\},
\end{aligned} \tag{III.21}$$

$$\begin{aligned}
\tilde{\omega} = & \int \frac{d^4 l}{(2\pi)^4} \frac{1}{4 \sin^2 l/2} \sum_{\mu} \left[\cos^2 \frac{l_{\mu}}{2} (w_0 - W) \tilde{G}_R - \sin^2 \frac{l_{\mu}}{2} (w_0 - W) \tilde{G}_R \right. \\
& \left. + \frac{1}{2} \sin^2 l_{\mu} (\tilde{G}_L + \tilde{G}_R) \right],
\end{aligned} \tag{III.22}$$

$$\begin{aligned}
\sigma_m = & \int \frac{d^4 l}{(2\pi)^4} \frac{1}{4 \sin^2 l/2} \frac{1}{(1 - w_0 e^{-\alpha})^2} \sum_{\mu} \left[-\cos^2 \frac{l_{\mu}}{2} \frac{1 - e^{-\alpha} W}{1 - e^{\alpha} W} \right. \\
& \left. + r^2 \sin^2 \frac{l_{\mu}}{2} e^{-2\alpha} + r \sin^2 l_{\mu} \frac{e^{-\alpha}}{1 - e^{\alpha} W} \right] - 4 \int \frac{d^4 l}{(2\pi)^4} \frac{1}{(l^2)^2} \theta(\pi^2 - l^2).
\end{aligned} \tag{III.23}$$

The propagators \tilde{G}_L and \tilde{G}_R are defined by

$$\tilde{G}_L = \frac{1 - w_0^2}{2W \sinh \alpha} \left[\frac{\sinh \alpha_0 - \sinh \alpha}{2w_0 \sinh \alpha_0 (\cosh \alpha_0 - \cosh \alpha)} - \frac{e^\alpha - W}{e^{-\alpha} - W} \frac{1}{(e^\alpha - w_0)^2} \right], \quad (\text{III.24})$$

$$\tilde{G}_R = \frac{1 - w_0^2}{2W \sinh \alpha} \left[\frac{\sinh \alpha_0 - \sinh \alpha}{2w_0 \sinh \alpha_0 (\cosh \alpha_0 - \cosh \alpha)} - \frac{1}{(e^\alpha - w_0)^2} \right] \quad (\text{III.25})$$

with $e^{-\alpha_0} = w_0$. It should be noted that there is no additive mass correction in Eq. (III.17). Although the fermion self energy $\Sigma(p, m)_{st}$ has an additive mass correction, it vanishes in Σ_q because of the relation,

$$(w_0^{N-s} P_+ + w_0^{s-1} P_-) (W_1^+ P_+ + W_1^- P_-)_{st} (w_0^{N-t} P_- + w_0^{t-1} P_+) = 0, \quad (\text{III.26})$$

which has been shown in the previous paper [5]¹.

The full quark propagator at 1-loop level now becomes

$$\begin{aligned} S_q(p)_{\text{full}} &= \frac{1 - w_0^2}{i\cancel{p} + (1 - w_0^2)m} \left[1 + \Sigma_q(p, m) \frac{1 - w_0^2}{i\cancel{p} + (1 - w_0^2)m} \right] \\ &= \frac{1 - w_0^2}{i\cancel{p} + (1 - w_0^2)m - (1 - w_0^2)\Sigma_q(p, m)} + O(g^4), \end{aligned} \quad (\text{III.27})$$

and finally we obtain

$$S_q(p)_{\text{full}} = \frac{(1 - w_0^2)Z_w Z_2}{i\cancel{p} + (1 - w_0^2)Z_w Z_m^{-1}m} \quad (\text{III.28})$$

with

$$Z_2 = 1 + \frac{g^2 C_F}{16\pi^2} (\log \lambda^2 a^2 + \Sigma_1), \quad (\text{III.29})$$

$$Z_w = 1 - \frac{2w_0}{1 - w_0^2} \frac{g^2 C_F}{16\pi^2} \Sigma_3 = 1 + \frac{g^2 C_F}{16\pi^2} z_w, \quad (\text{III.30})$$

$$Z_m^{-1} = 1 + \frac{g^2 C_F}{16\pi^2} (-3 \log \lambda^2 a^2 - \Sigma_2 + \Sigma_1). \quad (\text{III.31})$$

From this relation we can see that Σ_3 is an additive renormalization to w_0 ,

$$(1 - w_0^2) Z_w = 1 - \left(w_0 + \frac{g^2 C_F}{16\pi^2} \Sigma_3 \right)^2. \quad (\text{III.32})$$

If we employ the mean-field (tadpole) improvement [8], we can write

$$S_q(p) = \frac{(1 - (w_0^{\text{MF}})^2)Z_w^{\text{MF}} u^{-1} Z_2^{\text{MF}}}{i\cancel{p} + (1 - (w_0^{\text{MF}})^2)Z_w^{\text{MF}} (u Z_m^{\text{MF}})^{-1} m}, \quad (\text{III.33})$$

¹ At finite N we need a few extra terms for the renormalization such as an additive mass counter term. However these terms always contain the factor $e^{-\alpha N}$ and can be suppressed in the large N limit before taking the continuum limit.

where $u = 1 - g^2 C_F T / 2$, $w_0^{\text{MF}} = w_0 - 4(u - 1)$,

$$Z_2^{\text{MF}} = 1 + \frac{g^2 C_F}{16\pi^2} \left(\log \lambda^2 a^2 + \Sigma_1 - 16\pi^2 \frac{T}{2} \right), \quad (\text{III.34})$$

$$Z_w^{\text{MF}} = 1 - \frac{2w_0}{1-w_0^2} \frac{g^2 C_F}{16\pi^2} \left(\Sigma_3 - 16\pi^2 \cdot 2T \right) \equiv 1 + \frac{g^2 C_F}{16\pi^2} z_w^{\text{MF}}, \quad (\text{III.35})$$

$$(Z_m^{\text{MF}})^{-1} = 1 + \frac{g^2 C_F}{16\pi^2} \left(-3 \log \lambda^2 a^2 - \Sigma_2 + \Sigma_1 - 16\pi^2 \frac{T}{2} \right). \quad (\text{III.36})$$

Of course equalities that $u Z_2 = Z_2^{\text{MF}}$, $(1 - w_0^2) Z_w = (1 - (w_0^{\text{MF}})^2) Z_w^{\text{MF}}$ and $Z_m = u Z_m^{\text{MF}}$ hold up to $O(g^4)$ terms.

In the continuum we employ the $\overline{\text{MS}}$ scheme with naive dimensional regularization. The one-loop self-energy in the continuum has the same form as (III.17) with, however, the replacements,

$$\log(\lambda a)^2 \rightarrow \log(\lambda/\mu)^2, \quad (\text{III.37})$$

$$\Sigma_1 \rightarrow \Sigma_1^{\overline{\text{MS}}} = 1/2, \quad (\text{III.38})$$

$$\Sigma_2 \rightarrow \Sigma_2^{\overline{\text{MS}}} = -2, \quad (\text{III.39})$$

$$w_0 \rightarrow 0. \quad (\text{III.40})$$

Let us define the quark wave function renormalization factor needed for converting the lattice field to the continuum field in the $\overline{\text{MS}}$ scheme by

$$q^{\overline{\text{MS}}} = (1 - w_0^2)^{-1/2} Z_w^{-1/2} \sqrt{Z_2(\mu a)} q^{\text{lat}}. \quad (\text{III.41})$$

To one-loop order we finally find that

$$Z_2(\mu a) = 1 + \frac{g^2}{16\pi^2} C_F \left[-\log(\mu a)^2 + z_2 \right], \quad (\text{III.42})$$

where

$$z_2 = \Sigma_1^{\overline{\text{MS}}} - \Sigma_1, \quad (\text{III.43})$$

and Z_w is given in (III.30). The quark mass renormalization factor defined by

$$m^{\overline{\text{MS}}}(\mu) = (1 - w_0^2) Z_w Z_m(\mu a) m \quad (\text{III.44})$$

is given by

$$Z_m(\mu a) = 1 + \frac{g^2}{16\pi^2} C_F \left[-3 \log(\mu a)^2 + z_m \right] \quad (\text{III.45})$$

with

$$z_m = (\Sigma_2^{\overline{\text{MS}}} - \Sigma_2) - (\Sigma_1^{\overline{\text{MS}}} - \Sigma_1). \quad (\text{III.46})$$

IV. RENORMALIZATION FOR QUARK BILINEAR OPERATORS

We consider quark bilinear operators in the following form

$$\mathcal{O}_\Gamma(x) = \bar{q}(x)\Gamma q(x), \quad \Gamma = 1, \gamma_5, \gamma_\mu, \gamma_\mu\gamma_5, \sigma_{\mu\nu}. \quad (\text{IV.1})$$

We calculate the one loop correction to the Green's function $\langle \mathcal{O}_\Gamma(x)q(y)\bar{q}(z) \rangle$ for massless quark with external momenta $p = p' = 0$, whose diagram is shown in Fig. 3. As in the previous section we notice that the external line is essentially written in terms of the quark propagator times dumping factors, (III.5) and (III.6). Making use of this fact the one loop full Green's function for small external momentum becomes

$$\langle (\bar{q}\Gamma q) \cdot q\bar{q} \rangle_{\text{full}} = \frac{(1 - w_0^2) Z_w Z_2}{i\cancel{p}} T_\Gamma \Gamma \frac{(1 - w_0^2) Z_w Z_2}{i\cancel{p}'}, \quad (\text{IV.2})$$

where T_Γ is given by

$$T_\Gamma = 1 + \frac{g^2 C_F}{16\pi^2} \left(-\frac{h_2(\Gamma)}{4} \log \lambda^2 a^2 + V_\Gamma \right) \quad (\text{IV.3})$$

with a Γ dependent constant $h_2(\Gamma) = 4(A), 4(V), 16(P), 16(S), 0(T)$. The finite renormalization factor V_Γ is given by

$$V_\Gamma = \frac{h_2(\Gamma)}{4} \log \pi^2 + I_\Gamma \cdot 16\pi^2, \quad (\text{IV.4})$$

$$I_\Gamma = \int \frac{d^4 l}{(2\pi)^4} \left[r^2 \sin^2 \frac{l}{2} + r \frac{\sin^2 l}{e^{-\alpha} - W} + \frac{A_\Gamma}{(e^{-\alpha} - W)^2} \right] \frac{1}{(e^\alpha - w_0)^2} \frac{1}{4 \sin^2 \frac{l}{2}} \\ - \frac{h_2(\Gamma)}{4} \int \frac{d^4 l}{(2\pi)^4} \frac{1}{(l^2)^2} \theta(\pi^2 - l^2), \quad (\text{IV.5})$$

where

$$A_\Gamma = \begin{cases} \cos^2 \frac{l}{2} \sin^2 l & \Gamma = S, P \\ \left(\cos^2 \frac{l}{2} - 2 \cos^2 \frac{l_\alpha}{2} \right) \left(\sin^2 l - 2 \sin^2 l_\alpha \right) & \Gamma = V_\alpha, A_\alpha \\ \left(\cos^2 \frac{l}{2} - 2 \cos^2 \frac{l_\alpha}{2} - 2 \cos^2 \frac{l_\beta}{2} \right) \left(\sin^2 l - 2 \sin^2 l_\alpha - 2 \sin^2 l_\beta \right) & \Gamma = T_{\alpha\beta} \end{cases}, \quad (\text{IV.6})$$

$\sin^2 l = \sum_\mu \sin^2 l_\mu$ and $\cos^2 l/2 = \sum_\mu \cos^2 l_\mu/2$. The renormalization factor of quark bilinear operator is written as

$$Z_\Gamma^q = (1 - w_0^2) Z_w Z_2 T_\Gamma \equiv (1 - w_0^2) Z_w Z_\Gamma^{\text{lat}}, \quad (\text{IV.7})$$

$$Z_\Gamma^{\text{lat}} = 1 + \frac{g^2 C_F}{16\pi^2} \left[\left(1 - \frac{h_2(\Gamma)}{4} \right) \log \lambda^2 a^2 + V_\Gamma + \Sigma_1 \right]. \quad (\text{IV.8})$$

It is seen from (IV.6) that $Z_A = Z_V$ and $Z_P = Z_S$, which is expected to hold if the chiral symmetry exists and is indeed so in the continuum QCD.

In the continuum, the on-shell vertex function to one-loop order is given in the $\overline{\text{MS}}$ scheme by

$$T_{\Gamma}^{\overline{\text{MS}}} = 1 + \frac{g^2 C_F}{16\pi^2} \left(\frac{h_2(\Gamma)}{4} \log(\mu/\lambda)^2 + V_{\Gamma}^{\overline{\text{MS}}} \right) \quad (\text{IV.9})$$

with $V_{\Gamma}^{\overline{\text{MS}}} = -1/2(A), -1/2(V), 2(P), 2(S), 0(T)$ for the anti-commuting definition of γ_5 .

Combining the above results and including self-energy corrections, the relation between the continuum operator in the $\overline{\text{MS}}$ scheme and the lattice operator is given by

$$O_{\Gamma}^{\overline{\text{MS}}}(\mu) = (1 - w_0^2)^{-1} Z_w^{-1} Z_{\Gamma}(\mu a) (\bar{q} \Gamma q), \quad (\text{IV.10})$$

where

$$Z_{\Gamma}(\mu a) = 1 + \frac{g^2 C_F}{16\pi^2} \left[\left(\frac{h_2(\Gamma)}{4} - 1 \right) \log(\mu a)^2 + z_{\Gamma} \right], \quad (\text{IV.11})$$

and

$$z_{\Gamma} = z_{\Gamma}^{\overline{\text{MS}}} - z_{\Gamma}^{\text{lat}} \quad (\text{IV.12})$$

with

$$z_{\Gamma}^{\overline{\text{MS}}} = V_{\Gamma}^{\overline{\text{MS}}} + 1/2 = 0(A), 0(V), 5/2(P), 5/2(S), 1/2(T), \quad (\text{IV.13})$$

$$z_{\Gamma}^{\text{lat}} = V_{\Gamma} + \Sigma_1. \quad (\text{IV.14})$$

Here it should be mentioned that $z_m = -z_S$ and consequently $Z_m(\mu a) = Z_S(\mu a)^{-1}$, since $\sigma_m = I_S$ ($\Sigma_2 = -V_S$). To show this we use the relation

$$\frac{(e^{-\alpha} - W)(e^{\alpha} - W)}{(e^{-\alpha} - W)^2} = \frac{1 + W^2 - 2W \cosh \alpha}{(e^{-\alpha} - W)^2} = -\frac{\sin^2 l}{(e^{-\alpha} - W)^2}. \quad (\text{IV.15})$$

Note that the chiral Ward-Takahashi identities, if exact, implies the three equalities $z_S = z_P = -z_m$ and $z_V = z_A$, which is satisfied without fine tuning in the domain-wall QCD.

V. NUMERICAL RESULTS

To calculate momentum integrals appeared in the previous two sections numerically, two independent methods are employed, in order to check formulae and programs. In the first method the momentum integration is performed by a mode sum for a periodic box of a size L^4 after transforming the momentum variable through $p_{\mu} = q_{\mu} - \sin q_{\mu}$. We employ the size $L = 64$ for integrals. In the second method the momentum integration is carried out by the Monte Carlo routine VEGAS, using 20 samples of 1000000 points each. We found that the both result agrees very well.

We first present basic quantities Σ_1 , Σ_3 , $V_S (= V_P)$, $V_V (= V_A)$, and V_T in table I for several values of M . Here Σ_2 is omitted since $\Sigma_2 = -V_S$ holds exactly. The finite part of quark renormalization factors z_w and z_2 , are given in table II. Since $z_m = -z_S$ we omit it here again. We also give mean-field improved values where M should be replaced by $\tilde{M} = M + 4(u - 1)$. In table III we give our main result of this paper, $z_{S,P}$, $z_{V,A}$ and z_T , for several values of M . In these tables errors estimated from difference between two methods of the numerical integration are in the (right) next to the last digit of each value.

VI. CONCLUSION

In this paper we have calculated renormalization factors for quark bilinear operators in domain-wall QCD at 1-loop of the perturbation theory. We find that $z_S = z_P = -z_m$ and $z_V = z_A$, which suggest that the chiral Ward-Takahashi identity holds exactly without fine tuning at this order of the perturbation theory. Our numerical values for z_X with $X = 2, m, S, P, V, A, T$ are compared with those for the Wilson fermion action with and without mean-field improvement and clover fermion action with $c_{SW} = 1$, given in table IV. No data for clover fermion action with mean-field improvement is given here since c_{SW} itself is modified through the mean-field improvement. Finite parts z_X are rather large without mean-field improvement in all three fermion formulations, but they becomes smaller after the mean-field improvement is performed for the domain-wall fermion and Wilson fermion.

Peculiar feature of the domain-wall QCD in its renormalization is an appearance of the overlap factor $(1 - w_0^2)Z_w$ for the physical quark field. The problem here is that the 1-loop correction z_w becomes very large unless $|1 - M|$ is small. For example, at $M = 1.7$, which is the value used in the quenched simulation at $\beta = 6.0$ [4], from table II $z_w = 137.03$ without mean-field improvement. This 1-loop correction is huge, so we can not trust the perturbation theory. If mean-field improvement is made with $u = P^{1/4}$ where P is the expectation value of the plaquette and is 0.59374 at $\beta = 6.0$, $z_w = 0.1893$ at $\widetilde{M} \simeq 1.2$. This value is reasonably small. This example suggests that one have to employ the mean-field improvement for perturbative renormalization factors in domain-wall QCD to convert the lattice result to the one in the $\overline{\text{MS}}$ scheme.

ACKNOWLEDGEMENTS

This work is supported in part by the Grants-in-Aid for Scientific Research from the Ministry of Education, Science and Culture (Nos. 2373, 2375). Y. T. and T. I are supported by Japan Society for Promotion of Science.

REFERENCES

- [1] Y. Shamir, *Nucl. Phys.* **B406** (1993) 90.
- [2] V. Furman and Y. Shamir, *Nucl. Phys.* **B439** (1995) 54.
- [3] D. B. Kaplan, *Phys. Lett.* **B288** (1992) 342.
- [4] T. Blum and A. Soni, *Phys. Rev.* **D56** (1997) 174 ; hep-lat/9706023 ; hep-lat/9712004 .
- [5] S. Aoki and Y. Taniguchi, hep-lat/9711004 (to appear in PRD).
- [6] T. Blum, A. Soni and M. Wingate, hep-lat/9809065.
- [7] R. Narayanan and H. Neuberger, *Phys. Lett.* **B302** (1993) 62.
- [8] G. P. Lepage and P. Mackenzie, *Phys. Rev.* **D48** (1993) 2250.

TABLES

TABLE I. Value of Σ_1 , Σ_3 and V_T .

M	Σ_1	Σ_3	$V_{S,P}$	$V_{V,A}$	V_T
0.050	13.25	51.22	3.30	4.833	5.344
0.100	13.16	51.05	3.82	4.835	5.173
0.150	13.08	50.89	4.24	4.836	5.035
0.200	13.01	50.74	4.60	4.837	4.915
0.250	12.94	50.61	4.93	4.838	4.807
0.300	12.88	50.49	5.24	4.840	4.707
0.350	12.83	50.37	5.53	4.84	4.613
0.400	12.77	50.27	5.80	4.84	4.524
0.450	12.72	50.17	6.06	4.85	4.439
0.500	12.68	50.07	6.31	4.85	4.357
0.550	12.63	49.98	6.56	4.85	4.277
0.600	12.59	49.90	6.80	4.85	4.199
0.650	12.56	49.83	7.04	4.85	4.122
0.700	12.52	49.76	7.28	4.85	4.045
0.750	12.49	49.69	7.52	4.86	3.970
0.800	12.46	49.63	7.75	4.86	3.894
0.850	12.44	49.58	7.99	4.86	3.819
0.900	12.41	49.53	8.23	4.86	3.743
0.950	12.39	49.49	8.47	4.87	3.666
1.000	12.38	49.46	8.71	4.87	3.588
1.050	12.36	49.43	8.96	4.87	3.509
1.100	12.35	49.41	9.22	4.88	3.429
1.150	12.34	49.39	9.48	4.88	3.346
1.200	12.34	49.39	9.75	4.88	3.261
1.250	12.34	49.39	10.02	4.89	3.173
1.300	12.35	49.40	10.31	4.89	3.082
1.350	12.36	49.42	10.62	4.89	2.987
1.400	12.37	49.45	10.93	4.90	2.888
1.450	12.39	49.49	11.27	4.90	2.783
1.500	12.42	49.54	11.62	4.91	2.673
1.550	12.45	49.61	12.00	4.92	2.555
1.600	12.49	49.69	12.40	4.92	2.428
1.650	12.54	49.80	12.84	4.93	2.292
1.700	12.60	49.92	13.31	4.94	2.142
1.750	12.68	50.07	13.84	4.94	1.978
1.800	12.77	50.25	14.42	4.95	1.793
1.850	12.87	50.46	15.09	4.96	1.582
1.900	13.00	50.72	15.88	4.97	1.334
1.950	13.15	51.03	16.84	4.98	1.027

TABLE II. Value of z_2 and z_w . Mean-field improved values are also listed.

M	z_2	z_w	MF	
			z_2	z_w
0.050	-12.75	-998.23	-0.52	-44.70
0.100	-12.66	-483.60	-0.43	-20.05
0.150	-12.58	-311.75	-0.35	-11.99
0.200	-12.51	-225.53	-0.28	-8.057
0.250	-12.44	-173.52	-0.21	-5.759
0.300	-12.38	-138.59	-0.15	-4.272
0.350	-12.33	-113.39	-0.09	-3.244
0.400	-12.27	-94.248	-0.04	-2.502
0.450	-12.22	-79.114	0.01	-1.946
0.500	-12.18	-66.762	0.06	-1.521
0.550	-12.13	-56.408	0.10	-1.188
0.600	-12.09	-47.526	0.14	-0.9253
0.650	-12.06	-39.748	0.18	-0.7147
0.700	-12.02	-32.807	0.21	-0.5446
0.750	-11.99	-26.503	0.24	-0.4062
0.800	-11.96	-20.681	0.27	-0.2929
0.850	-11.94	-15.217	0.30	-0.1995
0.900	-11.91	-10.007	0.32	-0.1218
0.950	-11.89	-4.9617	0.34	-0.05631
1.000	-11.88	0.0	0.36	0.0
1.050	-11.86	4.9553	0.37	0.04993
1.100	-11.85	9.9813	0.38	0.09620
1.150	-11.84	15.159	0.39	0.1416
1.200	-11.84	20.577	0.39	0.1893
1.250	-11.84	26.339	0.39	0.2428
1.300	-11.85	32.569	0.39	0.3066
1.350	-11.86	39.420	0.38	0.3863
1.400	-11.87	47.091	0.36	0.4894
1.450	-11.89	55.846	0.34	0.6264
1.500	-11.92	66.053	0.32	0.8119
1.550	-11.95	78.235	0.28	1.068
1.600	-11.99	93.173	0.24	1.427
1.650	-12.04	112.09	0.19	1.945
1.700	-12.10	137.03	0.13	2.711
1.750	-12.18	171.66	0.05	3.895
1.800	-12.27	223.31	-0.03	5.840
1.850	-12.37	309.12	-0.14	9.357
1.900	-12.50	480.47	-0.26	16.91
1.950	-12.65	994.48	-0.42	40.95

TABLE III. Value of z_T . Mean-field improved values are also listed.

M				MF		
	$z_{S,P} = -z_m$	$z_{V,A}$	z_T	$z_{S,P} = -z_m$	$z_{V,A}$	z_T
0.050	-14.05	-18.083	-18.09	-1.82	-5.8497	-5.86
0.100	-14.48	-17.996	-17.83	-2.25	-5.7627	-5.60
0.150	-14.82	-17.918	-17.62	-2.59	-5.6853	-5.38
0.200	-15.11	-17.848	-17.43	-2.88	-5.6149	-5.19
0.250	-15.38	-17.783	-17.25	-3.15	-5.5503	-5.02
0.300	-15.62	-17.723	-17.09	-3.39	-5.4906	-4.86
0.350	-15.85	-17.668	-16.94	-3.62	-5.4352	-4.71
0.400	-16.07	-17.617	-16.80	-3.84	-5.3838	-4.57
0.450	-16.28	-17.569	-16.66	-4.05	-5.3359	-4.43
0.500	-16.49	-17.524	-16.53	-4.26	-5.2913	-4.30
0.550	-16.70	-17.483	-16.41	-4.46	-5.2500	-4.18
0.600	-16.90	-17.444	-16.29	-4.67	-5.2117	-4.06
0.650	-17.10	-17.409	-16.18	-4.87	-5.1764	-3.95
0.700	-17.30	-17.377	-16.07	-5.07	-5.1440	-3.84
0.750	-17.51	-17.347	-15.96	-5.27	-5.1145	-3.73
0.800	-17.71	-17.321	-15.86	-5.48	-5.0879	-3.62
0.850	-17.92	-17.297	-15.75	-5.69	-5.0643	-3.52
0.900	-18.14	-17.277	-15.66	-5.91	-5.0437	-3.42
0.950	-18.36	-17.259	-15.56	-6.13	-5.0262	-3.33
1.000	-18.59	-17.245	-15.46	-6.35	-5.0119	-3.23
1.050	-18.82	-17.234	-15.37	-6.59	-5.0012	-3.14
1.100	-19.07	-17.226	-15.28	-6.84	-4.9935	-3.05
1.150	-19.32	-17.223	-15.19	-7.09	-4.9898	-2.96
1.200	-19.59	-17.223	-15.10	-7.35	-4.9900	-2.87
1.250	-19.87	-17.227	-15.01	-7.63	-4.9944	-2.78
1.300	-20.16	-17.236	-14.93	-7.93	-5.0034	-2.70
1.350	-20.47	-17.250	-14.84	-8.24	-5.0174	-2.61
1.400	-20.80	-17.270	-14.76	-8.57	-5.0368	-2.53
1.450	-21.16	-17.295	-14.67	-8.92	-5.0621	-2.44
1.500	-21.54	-17.327	-14.59	-9.30	-5.0941	-2.36
1.550	-21.95	-17.366	-14.51	-9.71	-5.1335	-2.27
1.600	-22.39	-17.414	-14.42	-10.16	-5.181	-2.19
1.650	-22.88	-17.471	-14.34	-10.65	-5.238	-2.10
1.700	-23.42	-17.539	-14.25	-11.18	-5.307	-2.01
1.750	-24.01	-17.620	-14.16	-11.78	-5.388	-1.92
1.800	-24.69	-17.716	-14.06	-12.46	-5.484	-1.83
1.850	-25.46	-17.831	-13.95	-13.23	-5.598	-1.72
1.900	-26.37	-17.968	-13.83	-14.14	-5.735	-1.60
1.950	-27.49	-18.135	-13.68	-15.26	-5.902	-1.45

TABLE IV. Value of z_X for Wilson and clover fermion actions.

	Wilson	Clover($c_{SW} = 1$)	Wilson(MF)
z_2	-12.852	-9.206	-0.619
z_m	12.953	19.311	0.719
z_S	-12.953	12.661	-0.72
z_P	-22.596	9.602	-10.363
z_V	-20.618	16.657	-8.385
z_A	-15.797	18.193	-3.564
z_T	-17.018	20.824	-4.785

FIGURES

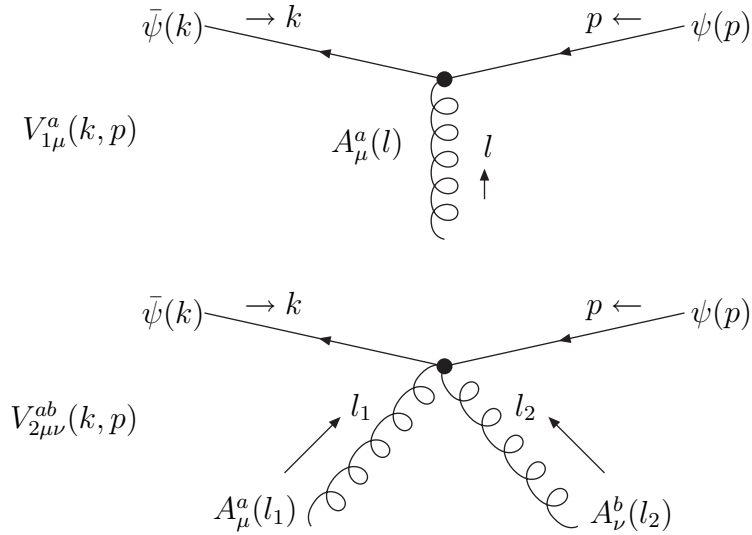


FIG. 1. Momentum assignment of the fermion-gluon vertices.

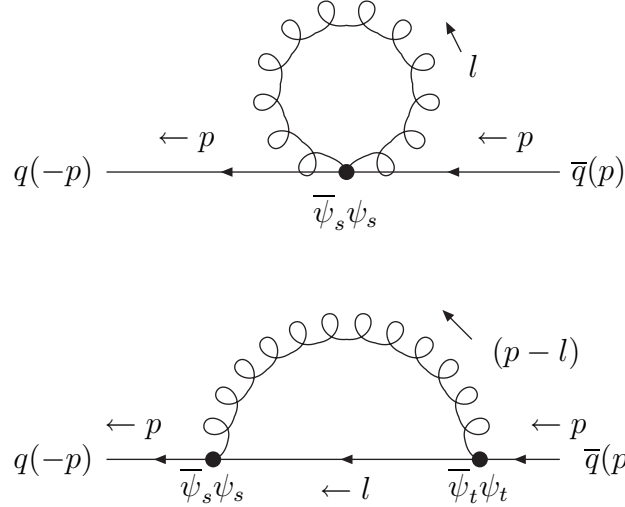


FIG. 2. One loop correction to the quark propagator.

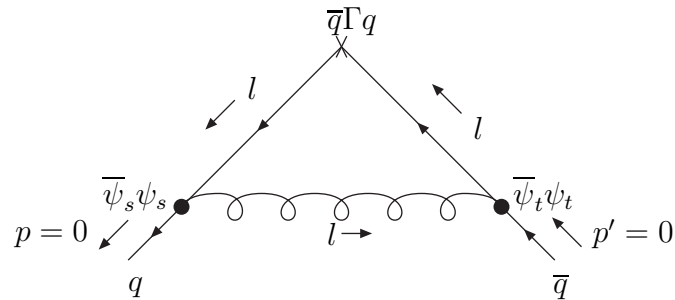


FIG. 3. One loop correction to the quark bilinear operator.